Exp Brain Res (2011) 208:491–505
DOI 10.1007/s00221-010-2496-8

RESEARCH ARTICLE

DTI-MR tractography of white matter damage in stroke patients with neglect

M. Urbanski · M. Thiebaut de Schotten · S. Rodrigo · C. Oppenheim · E. Touzé · J.-F. Méder · K. Moreau · C. Loeper-Jeny · B. Dubois · P. Bartolomeo

Received: 6 July 2010 / Accepted: 9 November 2010 / Published online: 27 November 2010

Abstract Left visual neglect is a dramatic neurological condition that impairs awareness of left-sided events. Neglect has been classically reported after strokes in the territory of the right middle cerebral artery. However, the precise lesional correlates of neglect within this territory remain discussed. Recent evidence strongly suggests an implication of dysfunction of large-scale perisylvian networks in chronic neglect, but the quantitative relationships between neglect signs and damage to white matter (WM) tracts have never been explored. In this prospective study, we used diffusion tensor imaging (DTI) tractography in twelve patients with a vascular stroke in the right hemisphere. Six of these patients showed signs of neglect. Non-parametric voxel-based comparisons between neglect and controls on fractional anisotropy maps revealed clusters in the perisylvian WM and in the external capsule. Individual DTI tractography identified specific disconnections of the fronto-parietal and fronto-occipital pathways in the neglect group. Voxel-based correlation statistics highlighted correlations between patients' performance on two visual search tasks and damage to WM clusters. These clusters were located in the anterior limb of the internal capsule and in the WM underlying the inferior frontal gyrus, along the trajectory of the anterior segment of the arcuate fasciculus (asAF). These results indicate that chronic visual neglect can result from, and correlate with, damage to fronto-parietal connections in the right hemisphere, within large-scale cortical networks important for orienting of spatial attention, arousal and spatial working memory.

Keywords Attention · Diffusion tensor imaging tractography · Hemispatial neglect · Stroke

Introduction

Vascular strokes in the right hemisphere often result in signs of neglect for events occurring on the left side of

Electronic supplementary material The online version of this article (doi:10.1007/s00221-010-2496-8) contains supplementary material, which is available to authorized users.

M. Urbanski (✉) · B. Dubois · P. Bartolomeo (✉)
INSERM-UPMC UMR S 975, G.H. Pitié-Salpêtrière,
47 boulevard de l'Hôpital, 75013 Paris, France
e-mail: marika.urbanski@gmail.com

P. Bartolomeo
e-mail: paolo.bartolomeo@upmc.fr

M. Thiebaut de Schotten
Natbrainlab, Department of Forensic and Neurodevelopmental Sciences, Institute of Psychiatry, King's College London, London, UK

S. Rodrigo · C. Oppenheim · J.-F. Méder
Department of Neuroradiology, Hôpital Sainte-Anne, Université Paris Descartes, Paris, France

E. Touzé
Department of Neurology, Hôpital Sainte-Anne, Université Paris Descartes, Paris, France

M. Urbanski · K. Moreau · C. Loeper-Jeny
Department of Functional Rehabilitation, Hôpital National de Saint-Maurice, Saint-Maurice, France

B. Dubois · P. Bartolomeo
Department of Neurology, AP-HP, IFR 70, Hôpital de la Salpêtrière, Paris, France

P. Bartolomeo
Department of Psychology, Catholic University, Milan, Italy

patients' space. Neglect patients seem to live in a halved world: they do not eat from the left part of their dish, or bump their body into obstacles situated on their left. When reproducing a linear drawing, they fail to copy the left part of the whole scene or of objects therein. On the other hand, patients' gaze tends to be captured by right-sided, ipsilesional objects, as if they exerted a sort of "magnetic" attraction (Gainotti et al. 1991). Besides its obvious interest for the cognitive neuroscience of visual attention and spatial processing, a better understanding of visual neglect is important on clinical grounds. In particular, post-stroke functional recovery is often poor in these patients (Malhotra et al. 2006) despite available rehabilitation procedures (Pisella et al. 2006) and promising possibilities for pharmacological treatments (Coulthard et al. 2008).

In the great majority of cases, lesions associated with neglect are localised in the territory of the middle cerebral artery (Husain and Nachev 2007; Mort et al. 2003). To identify the precise lesional correlate of neglect, studies have most often used the lesion overlapping method: the lesions of patients with neglect are superimposed in a referential space, lesions of brain-damaged patients without signs of neglect are subtracted out and the locus of maximum overlapping is considered as the critical region whose damage produces neglect. These studies reported hotspots in several distinct cortical loci: the angular gyrus in the inferior parietal lobule (Mort et al. 2003), portions of the angular and supramarginal gyri at the junction with the temporal lobe (Vallar 2001), more rostral portions of the superior temporal gyrus (Karnath et al. 2004), or the inferior frontal gyrus (Husain and Kennard 1996). Studies based on voxel-based lesion-symptom mapping (VLSM; see Bates et al. 2003) have also shown correlations between the involvement of the right inferior frontal gyrus and neglect signs (Committeri et al. 2007; Verdon et al. 2010). Thus, in most cases, lesions appear to cluster around a large perisylvian network in the right hemisphere (Mesulam 1981; Heilman et al. 1983; Bartolomeo 2006, 2007).

Signs of left neglect are likely to result from the interaction of spatial and non-spatial deficits (Bartolomeo 2007; Husain and Nachev 2007). Among these components, deficits of spatial attention have often been stressed (Posner et al. 1984; Losier and Klein 2001; Bartolomeo and Chokron 2002). fMRI evidence in normal participants indicate that orienting of spatial attention depends on the coordinated activity of fronto-parietal networks (Nobre 2001; Corbetta and Shulman 2002). In left neglect, left-hemisphere unimpaired networks show abnormal activity (Corbetta et al. 2005) and TMS-induced suppression of these networks ameliorates neglect (Koch et al. 2008). Neglect patients also often show non-lateralized deficits, such as an impairment of spatial working memory and reduced arousal (Husain and Rorden 2003).

In keeping with the multifarious nature of their symptoms, patients with neglect often have relatively large lesions, which are likely to disrupt several functional modules. If so, however, the lesion overlapping method, with its emphasis on focal hotspots, might not be conducive to accurate anatomo-clinical correlations. Moreover, the voxel-based statistics used by the lesion overlapping method relies on the "topological" assumption (Catani and Ffytche 2005) that the voxels of maximum overlap correspond to the crucial cortical correlate of the neurological deficit. While this may well be the case, it is also possible, according to a more "hodological" perspective, that lesions placed on different locations along the trajectory of a white matter pathway impair the integrated functioning of the cortical network connected by that pathway (Catani and Mesulam 2008). In this case, the lesion overlap method would be clearly inadequate to identify the brain network at issue. Along these lines, recent studies employed methods different from lesion overlapping to investigate the neural bases of neglect. Combining diffusion tensor imaging (DTI) tractography (Basser et al. 1994) with direct electrical stimulation of the brain (Duffau et al. 1999), Thiebaut de Schotten et al. (2005) showed that the temporary inactivation of the likely human homologue of the second branch of the superior longitudinal fasciculus (SLF II), a fronto-parietal white matter pathway (Schmahmann and Pandya 2006), can provoke transitory signs of left neglect. This evidence confirmed and specified the findings of Leibovitch et al. (1998) and Doricchi and Tomaiuolo (2003), who reported a maximum lesion overlap on the SLF in stroke patients with neglect. A maximum lesion overlap on white matter was also reported in the relatively rare cases of neglect after lesions in the territory of the right posterior cerebral artery (Mort et al. 2003; Park et al. 2006). The overlap location was compatible with the trajectory of the inferior longitudinal fasciculus (ILF; Bird et al. 2006). Using DTI tractography, Urbanski et al. (2008) performed in vivo reconstruction of the SLF, the ILF and a further long-range pathway running in the depth of the temporal lobe, the inferior fronto-occipital fasciculus (IFOF), in four patients with right brain lesions. DTI evidence of IFOF disconnection was present only in the two patients showing signs of left neglect.

Diffusion tensor imaging tractography has recently been used to obtain a detailed anatomical description of the white matter pathways connecting perisylvian brain areas in the left human hemisphere (Catani et al. 2005). There is a well-established direct pathway, the arcuate fasciculus (AF), connecting the Wernicke territory (including the posterior part of both the superior temporal gyrus, STg and middle temporal gyrus, MTg) with the Broca territory (Brodmann areas 44 and 45, and part of the middle frontal gyrus and inferior precentral gyrus). This long segment presents an asymmetry favouring the left hemisphere, perhaps

related to its role in language processes (Rodrigo et al. 2007). In addition, there is an indirect pathway consisting of two segments, a posterior segment (psAF) connecting Wernicke territory with the inferior parietal lobe (IPL), and a fronto-parietal or anterior segment (asAF) linking IPL with posterior Broca territory (compared to the projections of the AF), which likely corresponds to the human homologue of the third branch of the superior longitudinal fasciculus (SLF III; Schmahmann and Pandya 2006). However, DTI tractography showed that in the right hemisphere, the long segment appears to be present only in 40% of the normal population (Catani et al. 2007). Therefore, 60% of people seem to have only the asAF (connecting IPL and posterior Broca territory) and the psAF (connecting IPL and STg/MTg) in the right hemisphere (Catani et al. 2007). Interestingly, results of Catani et al.'s study (2007) indicated an inter-hemispheric difference in the structural organisation of the asAF, with higher fractional anisotropy (FA) values in the right hemisphere than in the left hemisphere, consistent with the possibility of a right-hemisphere ventral attentional network (VAN; Corbetta and Shulman 2002).

Indeed, besides their crucial role for language in the left hemisphere, these networks are also important for attentional processes. The right-hemisphere homologue of the network connected by asAF/SLF III and psAF is active when subjects reorient their attention from an expected location to an unexpected one (Corbetta and Shulman 2002). More dorsal areas in the posterior parietal cortex (PPC) and in the lateral prefrontal cortex (PFC), connected by more dorsal branches of the SLF (Schmahmann and Pandya 2006; Thiebaut de Schotten et al. 2008), are active during spatial orienting tasks (Nobre 2001; Corbetta and Shulman 2002). In particular, PPC activity is modulated by area 46 in the PFC (McIntosh et al. 1994; Büchel and Friston 1997). The human PPC (area 7 extending in the intraparietal sulcus) modulate responses in V5/MT area (analogue of area MT in the monkey) during attentional tasks (Friston and Büchel 2000). This suggests that the psAF has a role in synchronising activity in the dorsal visual pathway. By connecting parietal and temporal cortical modules, the posterior segment may also permit the time-locked integration of spatial and perceptual information that is necessary for attentional selection and conscious processing of visual objects (see Robertson 2003).

Concerning the white matter pathways ventral to the perisylvian regions, whose disconnection has also been implicated in neglect, the ILF is a ventral associative bundle with long and short fibres connecting the occipital and temporal lobes. The long fibres, which run medially to the short fibres, connect visual areas to the amygdala and the hippocampus (Catani and Thiebaut de Schotten 2008). The IFOF connects the ventro-lateral pre-frontal cortex and medial orbitofrontal cortex to the occipital lobe (Catani et al. 2002).

The optic radiations (OR), linking the lateral geniculate nucleus to the primary visual cortex, constitute a further white matter tract of interest in neglect, because their lesion can determine visual field defects. Homonymous hemianopia and visual neglect double dissociate in different patients. However, left hemianopia can interact with neglect in determining patients' performance, for example by dramatically increasing rightwards shifts of the subjective midpoint in line bisection (Doricchi and Angelelli 1999).

In view of these notions, it is important to explore the lesional correlates of neglect in stroke patients, by taking into proper account possible hodological determinants of neglect. To this aim, we obtained anatomical and DTI images in a group of 12 patients with right-hemisphere vascular lesions, six of whom showed signs of left neglect, and in 12 age-matched controls without neurological history. After traditional lesion overlapping, for each individual participant we performed a virtual in vivo dissection of the perisylvian networks, ILF, IFOF and OR. We subsequently combined tract dissection with a voxel-based approach (Ashburner and Friston 2000; Good 2001). Finally, we calculated the correlations between patients' performance on neuropsychological tests for neglect and DTI-based measures of structural integrity of the explored tracts.

Method

Participants

Twelve controls (6 women and 6 men; mean age 59.70 years, SD 7.52) without neurological history and twelve patients (4 women and 8 men) with a vascular stroke in the right hemisphere participated in this study. All participants were right handed and gave written informed consent. The ethics committee of the Hôtel-Dieu Hospital in Paris approved the protocol. Patients were consecutively included on the basis of inclusion and exclusion criteria. Inclusion criteria were as follows: age 18–80 years, presence of a unique stroke in the right hemisphere, absence of other white matter pathology (e.g. leukoaraiosis), time interval of at least 3 weeks between stroke onset and MRI. The exclusion criteria were the following: previous stroke, impaired comprehension, psychiatric disorders, altered vigilance, contraindications to MRI. Neglect was assessed using a paper-and-pencil neglect battery (Bartolomeo and Chokron 1999). Six patients presented signs of left visual neglect (N+) (63.75 years, SD 9.20), six other patients did not show any sign of neglect (N−) (58.77 years, SD 8.67). In the N+ group, the onset of stroke to time of neglect evaluation ranged from 9 to 2,187 days; in the N− group, the onset ranged from 5 to 571 days. Demographical, clinical

and neuropsychological data are reported in Table 1. Due to MRI inclusion criteria, time range between stroke onset and MRI was different in N+ and N− groups (20–2,187 days in the N+ group and 36–577 days in the N− group). There was no clinical evidence of neglect in the acute phase for N− patients. As it is often the case in these studies, neglect patients appeared to have larger lesion volume (mean, 88.38 cm^3; SD, 71.55) than non-neglect patients (mean, 16.52 cm3; SD, 18.36). However, the difference was not statistically reliable (Wilcoxon–Mann–Whitney test, $W = 93.5$, $P = 0.23$), probably as a consequence of the large variability in both groups.

Neuropsychological evaluation

The neglect battery included a line bisection test consisting in eight lines horizontally disposed in a vertical A4 sheet in a fixed random order (three 60 mm samples, three 100 mm

Table 1 Clinical and demographical data

	Lesion site	Visual field	Gender/age/education (years of schooling)	Onset of illness (days)	Line cancellation left/right hits (max 30/30)
N – 1	pI, STG, IPL, pMTOG	N	F/45/14	9	30/30
N – 2	pI, TP, STG, MTG, ITG	N	M/60/14	5	30/30
N – 3	F paraventricular, centrum semiovale	N	M/54/10	36	30/30
N – 4	Cuneus	LHH	M/69/12	571	30/30
N – 5	F paraventricular, pPutamen	N	M/58/12	177	30/30
N – 6	Infarct in the WM underlying the pars opercularis of the IFg	N	M/66/10	321	30/30
N + 1	T, O, rolandic, thalamo-capsular	LHH	M/64/10	2,187	17/30[a]
N + 2	Fus, H, I, TP, T, IFg, lenticular, thalamo-capsular, rolandic operculum, Precentral, Postcentral, SMg	LHH	M/66/8	65	0/16[a]
N + 3	T, P, frontal operculum, STS, IPL, MOG	LE	F/54/8	18	14/15[a]
N + 4	IPL, SPL, precuneus, cuneus, MTOG, pITG	LHH	F/80/17	729	30/30
N + 5	I, lenticular, F paraventricular	N	M/61/17	120	30/30
N + 6	Subinsular and temporal stem WM, BG, CR, IPL	LE	F/59/10	9	29/30

	Bells cancellation left/right hits (max 15/15)	Letter cancellation left/right hits (max 30/30)	Line bisection (% deviation)	Overlapping figures left/right hits (max 10/10)	Landscape drawing (max 6)
N − 1	15/15	29/30	−3.10	10/10	6
N − 2	15/15	28/29	4.80	10/10	6
N − 3	12/13	28/29	5.85	10/10	6
N − 4	15/15	29/29	−17.10[a,b]	10/10	6
N – 5	15/15	30/29	8.00	10/10	6
N – 6	15/15	30/30	0.24	10/10	6
N + 1	0/15[a]	1/22[a]	20.2[a]	9/10[a]	4.5[a]
N + 2	0/5[a]	0/22[a]	86.9[a,c]	2/5[a]	1[a]
N + 3	3/12[a]	15/25[a]	11.00	9/10[a]	4.5[a]
N + 4	1/15[a]	9/28[a]	1.00	9/10[a]	3.5[a]
N + 5	7/13[a]	29/30	14.20[a]	10/10	5[a]
N + 6	0/6[a]	0/13[a]	15.70[a]	6/10[a]	4.5[a]

[a] Pathological scores. For the line bisection test, cut-off at +11% deviation (Bartolomeo et al. 1994); for the bells cancellation, left–right difference >2 (Rousseaux et al. 2001); for the line cancellation, number of left omissions >1 (Albert 1973); for the letter cancellation, left–right difference >2; for the landscape drawing, score <6; for the overlapping figures, left omission >1 (Rousseaux et al. 2001). Visual fields: *N* normal, *LHH* left homonymous hemianopia, *LE* left extinction

[b] Leftward bias due to the compensation of LHH learned during rehabilitation procedures

[c] The 4 leftmost lines on the test sheet were omitted (see "Methods" for the corrected score of the deviation). *STg* superior temporal gyrus, *IPL* inferior parietal lobule, *pMTOg* posterior part of the middle temporo-occipital gyrus, *pI* posterior insula, *TP* temporal pole, *IFg* inferior frontal gyrus, *Fus* fusiform gyrus, *H* hippocampus, *MTg* middle temporal gyrus, *ITg* inferior temporal gyrus, *F* frontal, *SPL* superior parietal lobule, *pITg* posterior part of the inferior temporal gyrus, *T* temporal, *P* parietal, *STS* superior temporal sulcus, *BG* basal ganglia, *CR* corona radiata, *O* occipital, *I* insula, *WM* white matter

samples and two 180 mm samples; Bartolomeo et al. 1994); three cancellation tests in which patients were asked to cancel stimuli of various kind: (1) lines (Albert 1973), (2) As among other letters (Mesulam 1985), (3) silhouettes of bells among other objects (Gauthier et al. 1989); an overlapping figures task in which patients where requested to identify five patterns of overlapping linear drawings of common objects (one central and a pair of objects over each of its sides); a copy of a linear drawing representing a central house and four trees (a pair of trees over each of its side) presented on a horizontal A4 sheet. Visual fields and visual extinction were assessed using the confrontation task, which was administered following a previously described procedure (Bartolomeo and Chokron 1999).

Patients were considered to show left extinction when they failed to report at least one left visual stimulus occurring simultaneously with a right one; they were considered to show left hemianopia when they failed to report all left visual stimuli even on single hemifield stimulation. Diagnosis of neglect was based on pathological performance on at least 3 tests of the neglect battery. Patients were assigned to the non-neglect group when their performance was pathological on no more than one test of the neglect battery.

For the line bisection test, the cumulated percentage of deviation from the true centre for all the 8 lines was calculated. Rightward deviation assumed a positive sign (max +100), whereas leftward deviations carried a negative sign (max −100). Patient N + 2 (see Table 1) completely omitted to bisect the 4 leftmost lines in the test sheet. For these omitted lines, the deviation score was calculated as if the patient had put the bisection mark at the right endpoint of the line. For the landscape drawing, each completely copied tree was scored 1 point and the complete house 2 points. Items showing evidence of object-based neglect (i.e. only the right part of an item correctly drawn) received a score of 0.5 point (see Table 1).

For the correlation analyses between integrity of WM and performance to neuropsychological tests, we computed a laterality score (Bartolomeo and Chokron 1999) for the cancellation tests and for the overlapping figures test, which was entered as a regressor. This score is defined as $(x_1 - x_2)/(x_1 + x_2)$. Values for x_1 were given by the number of items cancelled (or reported for the overlapping figures task) on the right half of the page; values for x_2 corresponded to the number of left-sided cancelled items (or reported for the overlapping figures task). One advantage of this score is that it provides a quantitative estimate of spatial bias that is independent of the overall level of performance (e.g. of the total number of cancelled/reported targets). Its possible range is from −1 (all the items cancelled/reported on the left side, none on the right side) to +1 (the opposite situation). A correction was needed for cancellation tasks performed by patients with severe neglect, who cancelled only the rightmost items, without crossing the midline. In order not to underestimate their neglect, the laterality score obtained by these patients was augmented by the proportion of the number of neglected items on the right side (max +1.93, corresponding to a single bell cancelled on the right). For the line bisection test, the cumulated percentage of deviation for all the 8 lines was entered as a regressor (for patient N + 2, the percentage of deviation was corrected as shown above). For the landscape drawing, the score/6 was entered as a regressor.

Magnetic resonance imaging acquisition

An echo-planar imaging at 1.5T (General Electric) with a standard head coil for signal reception was used for all the acquisitions. High-resolution 3-D anatomical SPGR images were first acquired for each participant (114 axial contiguous images, 1.2 mm thick with a FOV of 28 cm).

DTI axial volumes were obtained using a repetition time of 6,575 ms with an echo time of 74.3 ms and a flip angle of 90°. Diffusion weighting images were performed along 36 independent directions, with a *b*-value of 700 s/mm^2. We used a slice thickness of 4 mm with no gap. The resolution of this acquisition sequence was 1.09 × 1.09, the matrix size was 256 × 256 with a FOV of 28 cm. The overall acquisition time took was 620 s.

Lesion analysis

An expert blind to the results of the neglect battery drew all lesions manually on slices of the T1 template from MRIcro software (http://www.mricro.com). Lesions for the N+ and N− groups were overlapped separately on the Colin27 (Holmes et al. 1998) registered in a stereotaxic space (Montreal Neurological Institute, MNI, http://www.mni.mcgill.ca/).

Tract-based analysis

Diffusion toolkit (http://www.trackvis.org/) computed the diffusion tensors for each subject and performed an interpolated streamline tractography for all voxels with an FA above an arbitrary threshold of 0.2. This threshold was chosen following two studies, which tested different thresholds with tractography of the cortico-spinal tract in patients with stroke (Kunimatsu et al. 2004) and the uncinate fasciculus in Alzheimer's disease (Taoka et al. 2009). An angle threshold of 45° was chosen in order to reduce artefactual reconstructions. We used a standard two-region of interest approach to isolate streamlines of the inferior longitudinal fasciculus (ILF), the inferior fronto-occipital fasciculus (IFOF), the posterior segment (psAF) and the anterior segment (asAF) of the arcuate fasciculus for the left and the right hemisphere (Catani et al. 2002, 2005; Catani and

Thiebaut de Schotten 2008). For all fasciculi except the optic radiations (OR), we placed spherical ROIs in each participant's FA map in the native space. For the OR, ROIs were manually drawn. For the psAF, the first ROI was placed caudally in the white matter underlying the Wernicke's territory (including the posterior part of both the STg and MTg) and the second ROI was placed in the white matter of the angular gyrus (Geschwind's territory; Catani et al. 2005, 2007). For the asAF/SLF III, the first ROI was placed in the white matter underlying Broca's territory (Brodmann areas 44 and 45, and part of the middle frontal gyrus and inferior precentral gyrus) and the second ROI was placed caudally including the white matter underlying the Geschwind's territory (Catani et al. 2005, 2007). For the ILF and the IFOF, the first ROI was placed in the occipital white matter: for the ILF, the second ROI was placed in the white matter underlying the rostral temporal regions (Catani et al. 2003), whereas for the IFOF, the second ROI was placed rostrally in the white matter of the anterior floor of the external capsule (Catani et al. 2002). Concerning the optic radiations (OR), a first coronal ROI was drawn in the posterior occipital lobe and the second ROI at the apex of the Meyer's loop (Ciccarelli et al. 2003; Thiebaut de Schotten et al. 2010). An example of the ROIs and the resulting tractography for each fasciculus in a representative subject from each group is given in the Supplementary Fig. 1.

Sizes of the ROIs were variable between subjects but did not differ significantly between groups of participants, whatever the tract of interest and the hemisphere (see Supplementary Fig. 2).

We extracted the number of streamlines for each subject and each reconstructed tract and calculated its 95% inferential confidence intervals (ICIs; Tryon 2001; Tryon and Lewis 2008) for the mean of each condition. The use of ICIs addresses some of the problems of traditional null hypothesis testing (Tryon 2001). The ICI method permits to infer statistical difference as well as equivalence by providing an intuitive graphic method (Tryon and Lewis 2008). Non-overlapping ICIs indicate statistical difference ($\alpha = 0.05$), whereas ICI overlap denotes statistical equivalence. Statistical indeterminacy occurs when both tests are failed.

Voxel-based analysis

Brainvisa 3.0.1 (http://www.brainvisa.info) created an FA map for each DTI. These maps were registered to the MNI space and smoothed with a full half width maximum (FWHM) of 11 mm following standard options provided in SPM5 (http://www.fil.ion.ucl.ac.uk/spm/).

Voxel-based statistics were performed by using the Statistical non Parametric Mapping toolbox (SnPM5b, http://www.sph.umich.edu/ni-stat/SnPM). SnPM5b computes voxel-by-voxel nonparametric two sample *t* tests (called pseudo *t*-statistic), by using a standard nonparametric multiple comparisons procedure based on randomisation/permutation testing (Holmes et al. 1996; Nichols and Holmes 2002). In the case of group comparisons, subjects cannot be assigned randomly, thus leading to make weak distribution assumptions (Nichols and Holmes 2002). The permutation test does not require any distributional assumption (Hayasaka and Nichols 2003) and is most suitable for designs with low degrees of freedom available for variance estimation (Salmond et al. 2002; Winkler et al. 2008). As FA maps have been shown to exhibit non-normality (Jones et al. 2005), the permutation approach has been recommended for voxelwise analysis of DTI data (Smith et al. 2007; Goodlett et al. 2009). We compared the three groups (controls, N−, N+) using pseudo *t*-statistics on the FA maps (1,000 permutations; smoothing of variance at 8 FWHM). The results were provided at $P < 0.05$ with a correction for multiple comparisons (FWE). We assessed the co-variation between the integrity of the white matter and performance on the neuropsychological tests (the scores for the cancellation tests, the overlapping figures test, the landscape drawing and the percentage of deviation for the line bisection test) with a simple nonparametric regression performed on the FA maps of twelve patients and six controls (three men and three women) who had performed the complete paper-and-pencil test battery. The nonparametric regression method implemented in SnPM5b does not assume any particular relationship between the variables (see Gosh et al. 2007) and permits permutations.

Tract overlap maps

For each tract of each control participant, a binary map was computed by assigning each pixel a value of 1 or 0 depending on whether the pixel was intersected by the tract (Ciccarelli et al. 2003; Thiebaut de Schotten et al. 2008). The 12 binary maps obtained for each tract were spatially normalised to the FA map computed in the voxel-based analysis. The maps were then summed in SPM5 (http://www.fil.ion.ucl.ac.uk/spm/) to produce overlap maps for each tract of interest.

Results

Lesion overlap

Overlay lesion plots of the N+ and the N− groups are represented in Fig. 1.

A first maximum lesion overlap (Fig. 1, yellow, 5/6 patients) in the N+ group was found in the right external capsule ($Z = -4$). The overlap extended to the grey matter and the white matter of the insula, the STg and the rolandic operculum ($Z = -4$ to 20). A second overlap ($Z = 28$) was in the superior paraventricular white matter (Fig. 1, green, 4/6 patients).

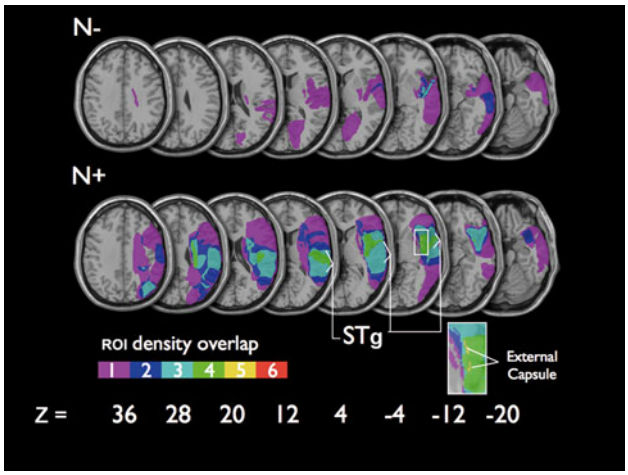

Fig. 1 N−: Overlay lesion plots of the patients with right brain damage without spatial neglect ($n = 6$); N+: Overlay lesion plots of the patients with spatial neglect ($n = 6$). The number of overlapping lesions is illustrated by the *colour bar* coding increasing frequencies from *violet* ($n = 1$) to *red* ($n = 6$). MNI z-coordinates of each transverse section are given. The *white rectangular* window zoomed at $z = -4$ shows a maximal overlap (5/6 N+) in the external capsule. *STg* Superior temporal gyrus

In the N− group, the lesions overlapped on the right insula and the right STg ($Z = -4$) in 3/6 patients, a region also found in the N+ group.

Tractography reconstruction

Figure 2 shows the mean track counts in the left and in the right hemisphere with 95% inferential confidence intervals (ICIs; Tryon 2001) for each subject group and each tracked fasciculus. In the left hemisphere, there was substantial ICI overlapping for N+, N− and controls, indicating statistical equivalence of the number of streamlines. The only exception was the asAF/SLF III in the N− group, where less streamlines were found in the left hemisphere than in the right hemisphere.

In the right hemisphere, ICIs showed substantial overlapping for the ILF, which resulted thus comparable in patients and controls. All neglect patients but N + 5 and N + 6 presented a disconnection of psAF, which resulted in large variability of track counts in the N+ group and consequent statistical indeterminacy. The neglect group differed significantly from both the N− and the control groups for three right hemisphere tracts: OR (patients N + 1, N + 2 and N + 4 had complete disconnection, consistent with their left homonymous hemianopia), IFOF (all N+ patients presented a complete disconnection) and asAF/SLF III (patients N + 1, N + 2, N + 3 and N + 5 had a disconnection of this tract).

Table 2 summarises for the neglect patients their performance to the neglect battery and the tracts disconnected.

Voxel-based analysis

Neglect patients had significantly lower FA level when compared to controls in the right hemisphere, in clusters (Fig. 3, blue) mostly localised in the white matter underlying the pars opercularis of the inferior frontal gyrus, the supramarginal gyrus, the middle temporal gyrus, the occipito-temporal white matter and the internal and the external capsules. Table 3 displays the relative coordinates in the MNI space. Comparison of right brain-damaged patients with and without neglect revealed a cluster of decreased FA in the white matter underlying the pars opercularis of the right IFg (MNI coordinates 34 8 22; Fig. 3, pink), in a region consistent with the trajectory of the asAF/SLF III are running through (see Fig. 4). When compared with controls, patients without neglect had decreased FA in the right

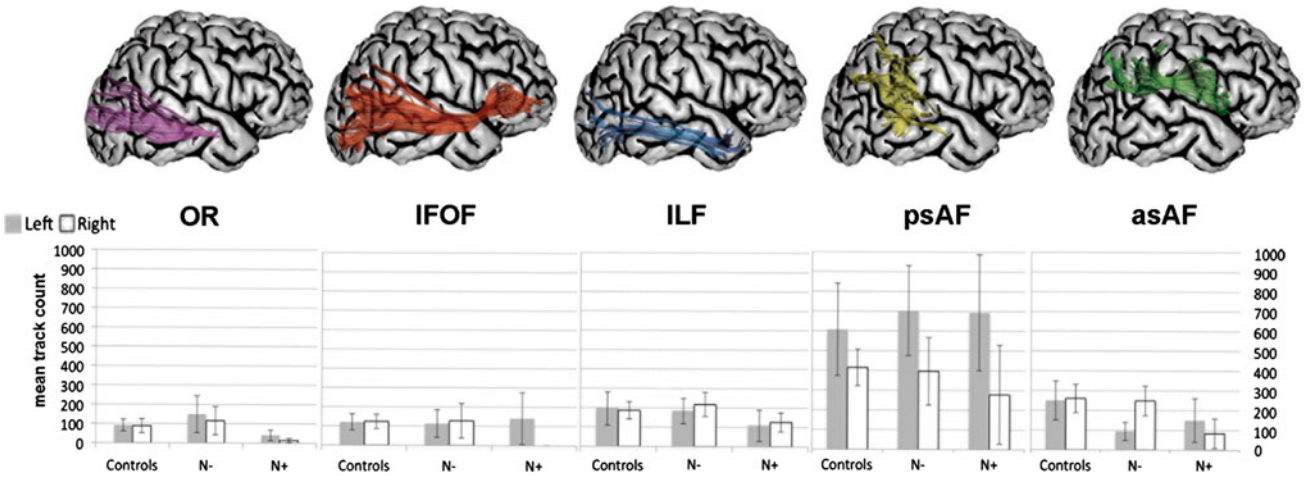

Fig. 2 Mean track counts with 95% inferential confidence intervals in the left (in *grey*) and the right hemisphere (in *white*) in each group of participants (Controls; N−, N+) for all fasciculi (OR; IFOF; ILF; psAF and asAF/SLFIII). An example of each fasciculus is shown in a 3D reconstruction of a brain

Table 2 Performance on the neglect battery and identification of the tract disconnected for each neglect patient

	Visual field	Line bisection	Bells cancel	Line cancel	Letter cancel	Overlap fig	Landscape drawing	Tract
N + 1	LHH	20.2[a]	0/15[a]	17/30[a]	1/22[a]	9/10[a]	4.5[a]	OR, IFOF, psAF, asAF
N + 2	LHH	86.9[a]	0/5[a]	0/16[a]	0/22[a]	2/5[a]	1[a]	OR, IFOF, psAF, asAF
N + 3	LE	11.00	3/12[a]	14/15[a]	15/25[a]	9/10[a]	4.5[a]	IFOF, psAF, asAF
N + 4	LHH	1.00	1/15[a]	30/30	9/28[a]	9/10[a]	3.5[a]	OR, IFOF, psAF
N + 5	N	14.20[a]	7/13[a]	30/30	29/30	10/10	5[a]	IFOF, asAF
N + 6	LE	15.70[a]	0/6[a]	29/30	0/13[a]	6/10[a]	4.5[a]	IFOF

[a] Pathological scores

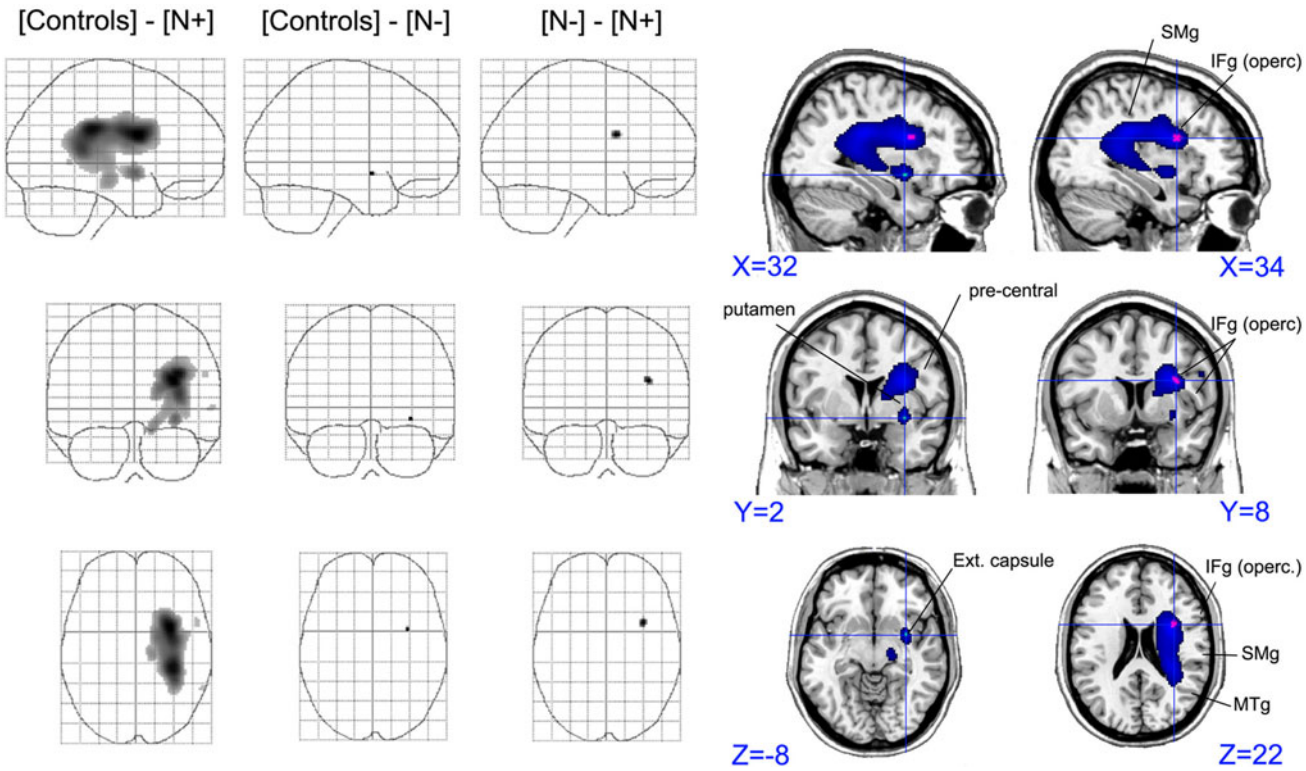

Fig. 3 Regions showing significantly reduced FA, in *Blue*, [Controls] vs. [N+]; in *Pink*, [N−] vs. [N+]; in *Green*, [Controls] vs. [N−] (all comparisons $P < 0.05$ FWE-corrected). The *left part* The left part of the figure corresponds to the sagittal, coronal and axial views of a glass brain representing the pseudo-*t* statistic in SnPM5b obtained for each comparison between groups of participants. The *right part* of the figure shows the overlap of the statistic maps onto a ch2 template of mricron (http://www.mricron.com) in the MNI coordinates (*X Y Z*) corresponding to the maximal pseudo-*t* values for the FA difference between [N+] and [N−] (34 8 22) and between [N−] and [Controls] (32 2 −8). IFg (operc.), pars opercularis of the inferior frontal gyrus. *MTg* Middle temporal gyrus, *SMg* supramarginal gyrus

external capsule (MNI coordinates 32 2 −8; Fig. 3, green). Table 4 displays for each patient (N+ and N−) the sparing or not of the clusters found in the voxel-based analysis.

Correlation with neglect signs

There was a significant nonparametric correlation (at $P < 0.05$, FWE-corrected) between reduced white matter integrity (FA maps) and neglect behaviour on the bells and the letter cancellation tests, whereas there was no correlation with the other tests of the neglect battery at this threshold. Figure 5 shows a cluster of statistical significance for the letter cancellation task (MNI coordinates: 18 6 6) ($k = 32$; Pseudo-$t = 6.20$, $P = 0.032$) and two further clusters for the bells cancellation, one localised in the white matter of the pars opercularis of the right inferior frontal gyrus (MNI coordinates: 28 10 28) ($k = 93$; Pseudo-$t = 6.10$, $P = 0.025$) and the other in the anterior limb of the right internal capsule (MNI coordinates: 18 4 8) ($k = 39$; Pseudo-$t = 5.88$, $P = 0.036$). Interestingly, this cluster was very close anatomically and statistically from the local maxima of the significant cluster obtained for the letter cancellation test (Pseudo-$t = 6.12$; see Fig. 5).

The correlation coefficient between the laterality score for the letter cancellation and the mean FA value in the

Table 3 White matter regions with significantly decreased FA in all comparisons (FWE-corrected)

	Coordinates			*k*	Pseudo-*t*
	x	*y*	*z*		
N+ vs. controls					
IFg (pars opercularis) WM	30	4	22	4,661	9.17***
SMg WM	34	−30	28		8.77***
Occipito-temporal WM	34	−40	12		7.68**
Internal capsule	18	0	10		5.66*
External capsule	32	2	−6	145	6.71**
Middle temporal gyrus	60	−50	2	7	4.90*
Inferior frontal gyrus (pars opercularis)	56	10	26	11	4.90*
N− vs. controls					
External capsule	32	2	−8	2	5.00*
N+ vs. N−					
IFg (pars opercularis) WM	34	8	22	20	5.54*

* $P < 0.05$; ** $P < 0.01$; *** $P < 0.001$

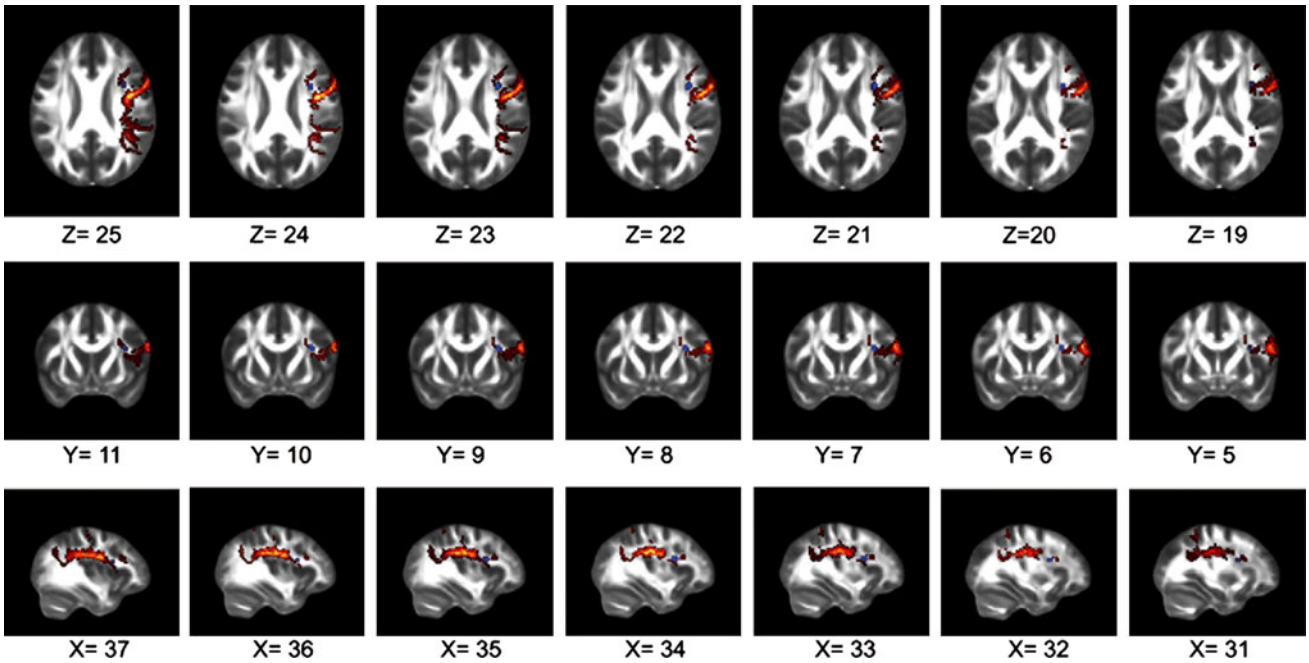

Fig. 4 Overlay onto a FA-MNI template of the asAF/SLFIII overlap map (in *yellow–red*; *yellow* corresponding to a higher degree of overlap) and of the cluster of statistical significance (MNI coordinates 34 8 22) obtained in SnPM5b for the comparison of [N+] vs. [N−] (in *blue*). Each slide comprising the cluster is presented in the axial ($Z = 19–25$), the coronal ($Y = 5–11$) and the sagittal ($X = 31–37$) planes

anterior limb of the right internal capsule (ALIC) was $R^2 = 0.73$; the correlation coefficients between the laterality score for the bells cancellation and the mean FA value in the ALIC was $R^2 = 0.68$ and $R^2 = 0.73$ for the mean FA value in the WM underlying the pars opercularis of the right IFg (see graphs at the bottom of Fig. 5).[1]

[1] These correlations should be interpreted with caution because they are calculated across groups with non-overlapping performance (with and without neglect) that may drive an artefactual correlation. However, visual inspection of the graphs in Fig. 5 shows that patients with more severe micro-structural damage tend to show more severe neglect on cancellation tests.

Discussion

This prospective study aimed at investigating the anatomical correlates of neglect signs in stroke patients. At variance with previous anatomical studies of neglect, mainly based on topological assumptions, we also took into account possible hodological factors in a small group of patients (Catani and Ffytche 2005). By using lesion overlapping, a method based on topological assumptions, we found a maximum overlap not in the cortex but in the white matter, consistent with many previous studies (Doricchi and Tomaiuolo 2003; Bird et al. 2006; Park et al. 2006;

Table 4 Examination of the clusters of FA difference obtained in the voxel-based analysis in the non-neglect and the neglect patients

	(30 4 22) IFg WM	(34 −30 28) SMg WM	(34 −40 12) O-T WM	(18 0 10) IC	(32 2 −6) EC	(60 −50 2) MTg	(56 10 26) IFg	(32 2 −8) EC	(34 8 22) IFg WM
N − 1	−/−	−/−	ab/+	−/−	−/−	+/+	−/ab	−/−	−/−
N − 2	−/−	−/−	+/+	−/−	−/−	ab/ab	ab/−	−/−	−/−
N − 3	ab/ab	ab/ab	−/−	−/−	−/−	−/−	−/−	−/−	ab/ab
N − 4	−/−	−/−	−/−	−/−	−/−	−/−	−/−	−/−	−/−
N − 5	−/−	−/−	−/−	−/−	−/−	−/−	−/−	−/−	−/−
N − 6	−/−	−/−	−/−	−/−	ab/ab	−/−	−/−	+/ab	−/−
N + 1	+/ab	+/+	+/+	+/+	+/+	+/ab	−/−	ab/+	ab/ab
N + 2	−/ab	+/+	+/+	+/+	+/ab	ab/+	+/+	+/ab	ab/ab
N + 3	+/+	+/ab	+/ab	−/−	ab/ab	+/+	ab/+	ab/ab	+/+
N + 4	−/−	ab/ab	+/+	−/−	−/−	ab/ab	−/−	−/−	−/−
N + 5	+/+	+/+	ab/+	−/−	ab/+	−/−	−/−	+/ab	ab/−
N + 6	+/+	ab/ab	−/−	−/−	+/+	−/−	−/−	+/+	ab/ab

MNI coordinates and localisation are displayed on the first raw. In each cell, the sparing or not of the cluster is mentioned on the T1/T2 MRI of each subject

− spared, + lesioned, *ab* abnormal appearing (usually in the vicinity of the lesion)

IFg WM White matter underlying the inferior frontal gyrus, *SMg WM* white matter underlying the supramarginal gyrus, *O-T WM* occipito-temporal white matter, *IC* internal capsule, *EC* external capsule, *MTg* middle temporal gyrus

Committeri et al. 2007; Golay et al. 2008; Verdon et al. 2010). In 3 of 6 patients without neglect, there was an overlap on the right insula and on the right superior temporal gyrus. This suggests that damage to these regions plays no crucial role in neglect.

Given the additional limitations of the lesion overlapping method in identifying networks and disconnections, we also employed DTI, a new technique that reveals the organisation of the white matter and its integrity. This method permits to establish anatomo-functional correlations based on white matter pathways. We chose to explore patients in a chronic stage, which prevented us from recruiting a large patient series.[2] However, despite the small number of patients in each group, voxel-based nonparametric statistics on the FA maps extracted from DTI demonstrated reduced structural integrity in the perisylvian white matter and external and internal capsules of the right hemisphere in neglect patients (Fig. 3). Damage to the internal capsule was probably related to persistent hemiplegia in the neglect group, especially for the upper limb (Behrens et al. 2003), whereas the lower limb partially recovered in 3/6 patients. Some of the clusters of FA difference revealed by the voxel-based analysis (Table 4) lied remotely to the lesion in the N+ group, presumably as a result of wallerian degeneration. Thus, voxel-based analysis of FA values permits to demonstrate WM disconnections lying far from the lesion, at variance with other methods (e.g. VLSM).

The virtual dissection of each individual tract allowed us to further specify the involved tracts within the perisylvian network revealed by the voxel-based approach. Individual tractography was performed using the ROIs described in the methods, on the axial individual FA maps. The asAF/SLF III resulted to be significantly involved in neglect patients, whereas the participation of the psAF was more variable, leading to statistical indeterminacy (Fig. 2). Concerning the external capsule area, which referred to more ventral networks, the IFOF, but not the ILF, was disconnected in our sample of neglect patients.

Fig. 5 Regions showing a significant correlation between the integrity of the white matter and the laterality scores for visual search tasks ($P < 0.05$ FWE-corrected). The statistic map was overlaid onto a ch2 template of mricron in the MNI coordinates corresponding to the maximal pseudo-*t* values. IFg (operc.), pars opercularis of the inferior frontal gyrus. *ALIC* Anterior limb of the internal capsule. Regression lines and correlation coefficient (R^2) between the laterality score obtained for the letter and the bells cancellation tests and the mean FA at the maximal pseudo-*t* values are represented in the graphs below each cluster of significant nonparametric regression; each non-neglect patient is represented by a *black star* and each neglect patient by a *blank diamonds*

[2] In order to avoid acute ischemic MRI artefacts such as cell swelling or cytotoxic oedema (see Sotak 2002), we established a minimum necessary time interval of 3 weeks between stroke and DT-MR acquisition; as a consequence, many patients tested behaviourally could not be included because they had left the hospital before any DTI sequence could be acquired. Time interval between stroke onset and MRI was chosen on the basis of several studies indicating an initial increase of FA at the acute stage due to cell swelling. At the sub-acute and chronic stages, there is a decreasing of FA in the lesion, due to wallerian degeneration (Thomalla et al. 2005). This decrease could remain significant (compared to the FA in the homologous controlateral lesion) even 6 months after the stroke (Sotak 2002). The second raison was the probability of frequent consecutive oedema at the acute stage, which could have disturbed the sensitivity of the DTI sequence to the lesion.

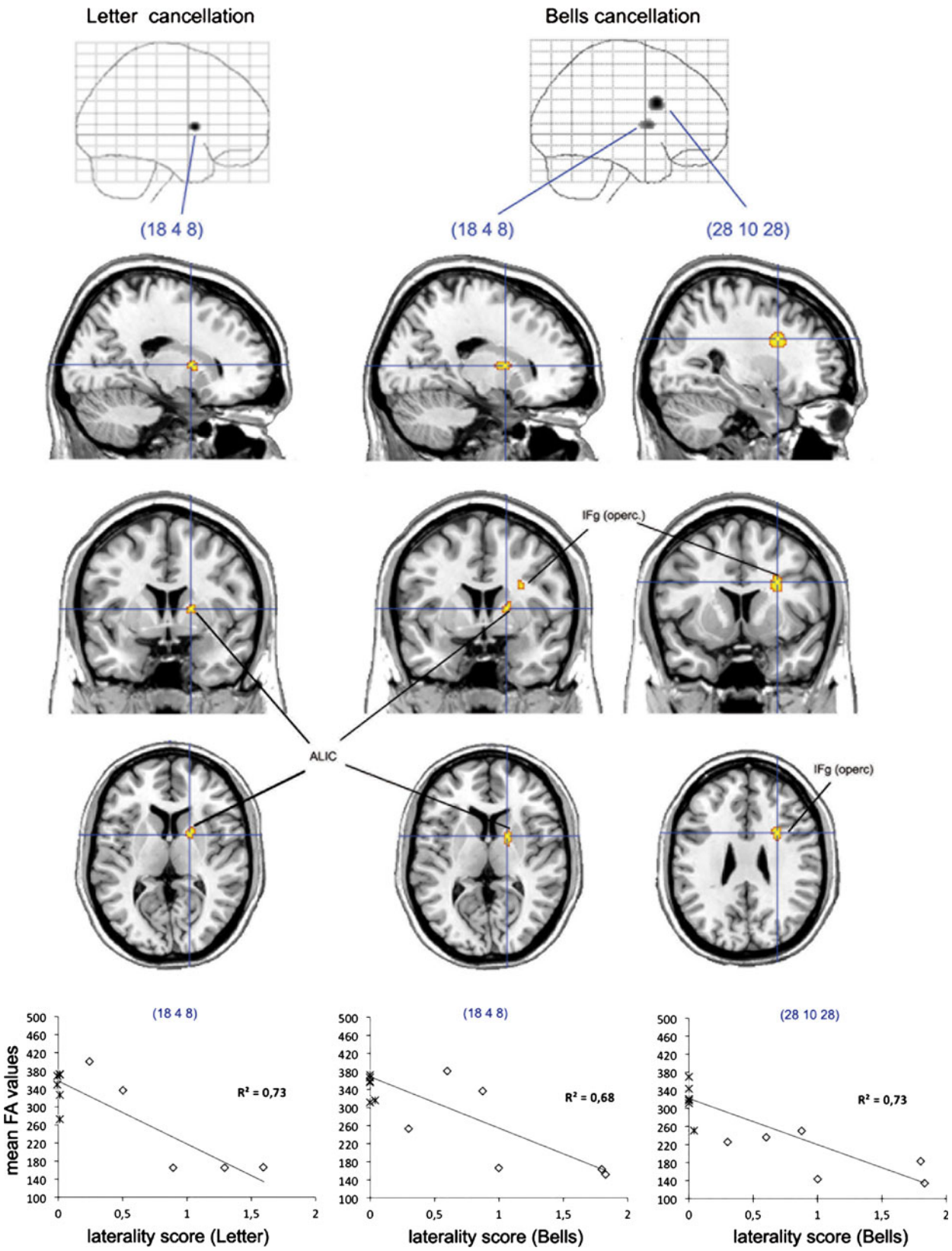
Letter cancellation
Bells cancellation
(18 4 8)
(18 4 8)
(28 10 28)
IFg (operc.)
ALIC
IFg (operc)
(18 4 8)
(18 4 8)
(28 10 28)
mean FA values
R² = 0,73
R² = 0,68
R² = 0,73
laterality score (Letter)
laterality score (Bells)
laterality score (Bells)

The OR were also damaged in neglect patients, consistent with the presence of homonymous hemianopia in half of our sample. Although hemianopia can dissociate from neglect signs, it can also worsen patients' performance when present (Doricchi and Angelelli 1999).

Disconnection of asAF/SLF III is consistent with accumulating evidence on the importance of SLF damage in neglect. This evidence comes from animal studies (Gaffan and Hornak 1997; Reep et al. 2004), from lesion overlap in stroke patients (Doricchi and Tomaiuolo 2003; Thiebaut de Schotten et al. 2008; Verdon et al. 2010) and from neurosurgical patients, who showed either transitory deficits upon temporary electrical inactivation of the SLF (Thiebaut de Schotten et al. 2005), or the occurrence or worsening of neglect signs after surgical interruption of the SLF (Shinoura et al. 2009).

The asAF/SLF III connects a ventral attentional network (VAN) network which shows BOLD responses in fMRI when participants have to respond to invalidly cued targets (Corbetta and Shulman 2002). The VAN might thus be responsible for reorienting of attention, whereas a more dorsal fronto-parietal pathway, the dorsal attentional network (DAN), probably linked by the human homologue of SLF II, would orient spatial attention during valid cueing. Corbetta et al. (2008) made the further proposal that the DAN, with possible contribution from other prefrontal regions such as the anterior cingulate and the anterior insula, filtrate the activation of the VAN and gate the sensory responses according to their behavioural relevance In neglect patients, damage to right-hemisphere VAN could cause a functional imbalance between the left and right DANs, with a hyperactivity of the left dorsal fronto-parietal network, which would provoke an attentional bias towards right-sided objects (Kinsbourne 1993) and neglect of left-sided items. Consistent with this hypothesis, suppressive TMS on the left parieto-motor pathway correlated with an improvement of patients' performance on cancellation tests (Koch et al. 2008). The IPL and its ventral frontal projections can also be responsible for maintaining attention on goal or task, which is a top-down process (Singh-Curry and Husain 2009). Impaired sustained attention combined with a deficit in detecting salient events after right hemispheric stroke may lead to an exacerbation of the spatial bias (Husain and Rorden 2003; Husain and Nachev 2007).

We previously described the involvement of the right IFOF in two neglect patients with predominantly subcortical lesion (Urbanski et al. 2008). This result was confirmed in the present sample, because the IFOF was disconnected in all patients with neglect and normal and symmetrical in all patients without neglect. Although damage to the IFOF might not be necessary by itself to produce signs of neglect [for example, the IFOF was intact in both the patients with neglect and SLF damage described by Shinoura et al. (2009)], it might contribute to neglect signs by depriving visual cortex of top-down modulation from more anterior regions, or by decreasing the influence of visual input on the right VLPFC, with consequent deterioration of patients' level of arousal (Doricchi et al. 2008; Urbanski et al. 2008) or sustained attention (see Singh-Curry and Husain 2009).

Several mechanisms of compensation, not mutually exclusive, are possible after white matter damage (Duffau 2009). These include the recruitment of redundant neurons located closely to the lesion; the recruitment of accessory contralesional pathways thanks to the suppression of callosal inhibition; the recruitment of parallel long-distance association pathways, whereby direct and indirect intrahemispheric pathways might compensate for each other. As a consequence, lesion volume, especially in the white matter, may be a critical factor of chronic neglect, by preventing these adaptive mechanisms to take place (Bartolomeo et al. 2007).

To obtain more quantitative estimates of the relationships between lesion sites and signs of neglect, we calculated non-parametric correlations between FA values and patients' performance on tests of the neglect battery. We found significant correlations between patients' scores on two paper-and-pencil tests, which required target/distractor discrimination (the letter and the bells cancellation tasks) and reduced structural integrity in the white matter in a common region consistent with the anterior limb of the internal capsule (Fig. 5). The anterior limb of the internal capsule contains the anterior thalamic radiations, a bundle of fibres linking anterior and dorsomedial thalamic nuclei with the prefrontal cortex and the cingulate gyrus, and fronto-pontine fibres (Crosby et al. 1962). Moreover, the performance in the bells cancellation correlated with another cluster in the white matter underlying the inferior frontal gyrus pars opercularis (Fig. 5), in a location consistent with the trajectory of the asAF/SLF III (Fig. 4). The right IFg, a cortical termination of the asAF/SLF III, has been implicated in signs of neglect when a target/distractor discrimination is needed (Husain and Kennard 1996), which was indeed the case with the bells cancellation test we employed. Interestingly, the recent study from Verdon et al. (2010) using a VLSM analysis on 80 patients with a right hemisphere stroke has shown that the factor (revealed by a prior factorial analysis on patients' performance to a battery of neglect tests) accounting for omission of targets in the bells cancellation test and in the Ota search task correlated with a peak in the right inferior frontal gyrus (BA 45) and in other prefrontal areas.

We found no significant correlation in our sample between line bisection performance and FA values. This pattern of results is consistent with the suggestion that patients with frontal or deep lesions may show neglect on cancellation task but perform normally on line bisection (Binder et al. 1992).

Patient N − 4 in the present series presented a pathological *leftward* bias in line bisection test, perhaps because of overcompensation (see Robertson et al. 1994). To test the hypothesis that the performance of this particular patient determined some of the observed correlations, we performed a further correlation analysis after having excluded patient N − 4. Voxel-based analysis still showed a difference in the FA integrity between controls and non-neglect patients located in the external capsule ($P < 0.05$, FWE-corrected), suggesting that this result was not driven by the location of the stroke in this patient. No correlation was found between reduced integrity of the white matter and performance to line bisection test, suggesting that the absence of correlation presented with all twelve patients was not driven by the pathological leftward deviation of this non-neglect patient. Moreover, correlation with both cancellation tests (letter and bells cancellation) was still present at $P < 0.05$, FWE-corrected, even after the exclusion of N − 4, in clusters localised very close to those described in the analyses performed with all patients.

Contrary to the present hodological approach to neglect anatomy, it has recently been argued that white matter damage is relatively unimportant in neglect. Using a probabilistic cytoarchitectonic atlas based on histological findings in 10 adult postmortem brains (Jülich atlas; Bürgel et al. 2006), Karnath et al. (2009) reanalysed their previously studied 140 right brain–damaged patients (78 with neglect and 62 without neglect) (Karnath et al. 2004), by combining the statistical lesion map obtained from the voxel-based lesion-behaviour mapping with the probabilistic cytoarchitectonic maps of the Jülich atlas. They showed that only 36.9% of the damaged voxels were in the white matter. Moreover, if damage to perisylvian pathways was typically found in neglect patients (especially in the superior occipito-frontal fasiculus, the SLF and the IFOF), the relationship between neglect signs and the involvement of these fasciculi was however not strongly predictive of neglect. However, as Bürgel et al. (2006) acknowledge, their atlas underestimate the tracts running rostro-caudally, including the fronto-parietal connections. Moreover, at variance to our study, Karnath and co-workers studied patients in the acute stage of their stroke. These issues limit the generality of the conclusions of the Karnath et al's reanalysis.

There are also limitations in our study. As mentioned before, the relatively large slice thickness may have increased partial volume effect, leading to false positives results in the voxel-based analysis and false negatives in the tractography reconstruction. Moreover, fibre crossing, kissing or fanning are limitations for the tensor model used in DTI to well reconstruct and visualise the trajectory of dorsal bundles such as the SLF I and SLF II. In areas with ischaemic injury, FA decreases after a few days in the perilesional areas (see Thomalla et al. 2005) leading to possible biased DTI-tractography reconstructions. We chose to study patients in the chronic stage of their infarcts to avoid this limitation, although adaptive mechanisms might have affected neglect deficits (but note that patients with acute infarcts can instead suffer from transient ischaemic penumbra in nearby areas and diaschisis phenomena in distant locations). Future studies based on a larger group of patients and new algorithms resolving multiple white matter orientations within voxels will be necessary to confirm and extent our analysis to supplementary tracts (Dell'acqua et al. 2010) and to understand the relationship between MRI signs of damage and severity of neglect.

In conclusion, this study is a first attempt to propose ways to explore causal relationship between network disconnection and visual neglect. The present results converge with accumulating previous evidence that signs of chronic left neglect can result from disruption of the coordinated activity of large-scale fronto-parietal networks in the right hemisphere.

Acknowledgments Supported by grants from the AP-HP (interface programme) and the Université Pierre et Marie Curie, Paris 6 (Bonus Qualité Recherche) to PB.

References

Albert ML (1973) A simple test of visual neglect. Neurology 23:658–664

Ashburner J, Friston KJ (2000) Voxel-based morphometry—the methods. NeuroImage 11:805–821

Bartolomeo P (2006) A parietofrontal network for spatial awareness in the right hemisphere of the human brain. Arch Neurol 63:1238–1241

Bartolomeo P (2007) Visual neglect. Curr Opin Neurol 20:381–386

Bartolomeo P, Chokron S (1999) Egocentric frame of reference: its role in spatial bias after right hemisphere lesions. Neuropsychologia 37:881–894

Bartolomeo P, Chokron S (2002) Orienting of attention in left unilateral neglect. Neurosci Biobehav Rev 26:217–234

Bartolomeo P, D'Erme P, Gainotti G (1994) The relationship between visuospatial and representational neglect. Neurology 44:1710–1714

Bartolomeo P, Thiebaut de Schotten M, Doricchi F (2007) Left unilateral neglect as a disconnection syndrome. Cereb Cortex 17:2479–2490

Basser PJ, Mattiello J, LeBihan D (1994) MR diffusion tensor spectroscopy and imaging. Biophys J 66:259–267

Bates E, Wilson S, Saygin A, Dick F, Sereno M, Knight RT, Dronkers N (2003) Voxel-based lesion-symptom mapping. Nat Neurosci 6:448–450

Behrens TE, Johansen-Berg H, Woolrich MW, Smith SM, Wheeler-Kingshott CA, Boulby PA, Barker GJ, Sillery EL, Sheehan K, Ciccarelli O, Thompson AJ, Brady JM, Matthews PM (2003) Non-invasive mapping of connections between human thalamus and cortex using diffusion imaging. Nat Neurosci 6:750–757

Binder JR, Marshall R, Lazar R, Benjamin J, Mohr JP (1992) Distinct syndromes of hemineglect. Arch Neurol 49:1187–1194

Bird C, Malhotra P, Parton A, Coulthard EJ, Rushworth MF, Husain M (2006) Visual neglect after right posterior cerebral artery infarction. J Neurol Neurosurg Psychiatr 77:1008–1012

Büchel C, Friston K (1997) Modulation of connectivity in visual pathways by attention: cortical interactions evaluated with structural equation modelling and fMRI. Cereb Cortex 7:768–778

Bürgel U, Amunts K, Hoemke L, Mohlberg H, Gilsbach JM, Zilles K (2006) White matter fiber tracts of the human brain: three-dimensional mapping at microscopic resolution, topography and intersubject variability. NeuroImage 29:1092–1105

Catani M, Ffytche D (2005) The rises and falls of disconnection syndromes. Brain 128:2224–2239

Catani M, Mesulam M (2008) The arcuate fasciculus and the disconnection theme in language and aphasia: history and current state. Cortex 44:953–961

Catani M, Thiebaut de Schotten M (2008) A diffusion tensor imaging tractography atlas for virtual in vivo dissections. Cortex 44:1105–1132

Catani M, Howard RJ, Pajevic S, Jones DK (2002) Virtual in vivo interactive dissection of white matter fasciculi in the human brain. NeuroImage 17:77–94

Catani M, Jones DK, Donato R, Ffytche D (2003) Occipito-temporal connections in the human brain. Brain 126:2093–2107

Catani M, Jones DK, Ffytche D (2005) Perisylvian language networks of the human brain. Ann Neurol 57:8–16

Catani M, Allin MP, Husain M, Pugliese L, Mesulam MM, Murray RM, Jones DK (2007) Symmetries in human brain language pathways correlate with verbal recall. Proc Natl Acad Sci USA 104:17163–17168

Ciccarelli O, Toosy AT, Parker GJ, Wheeler-Kingshott CA, Barker GJ, Miller DH, Thompson AJ (2003) Diffusion tractography based group mapping of major white-matter pathways in the human brain. NeuroImage 19:1545–1555

Committeri G, Pitzalis S, Galati G, Patria F, Pelle G, Sabatini U, Castriota-Scanderbeg A, Piccardi L, Guariglia C, Pizzamiglio L (2007) Neural bases of personal and extrapersonal neglect in humans. Brain 130:431–441

Corbetta M, Shulman G (2002) Control of goal-directed and stimulus-driven attention in the brain. Nat Rev Neurosci 3:215–229

Corbetta M, Kincade M, Lewis C, Snyder A, Sapir A (2005) Neural basis and recovery of spatial attention deficits in spatial neglect. Nat Neurosci 8:1603–1610

Corbetta M, Patel G, Shulman G (2008) The reorienting system of the human brain: from environment to theory of mind. Neuron 58:306–324

Coulthard EJ, Nachev P, Husain M (2008) Control over conflict during movement preparation: role of posterior parietal cortex. Neuron 58:144–157

Crosby EC, Humphrey T, Lauer EW (1962) Correlative anatomy of the nervous system. Macmillian Co., New York

Dell'Acqua F, Scifo P, Rizzo G, Catani M, Simmons A, Scotti G, Fazio F (2010) A modified damped Richardson–Lucy algorithm to reduce isotropic background effects in spherical deconvolution. NeuroImage 49:1446–1458

Doricchi F, Angelelli P (1999) Misrepresentation of horizontal space in left unilateral neglect: role of hemianopia. Neurology 52:1845–1852

Doricchi F, Tomaiuolo F (2003) The anatomy of neglect without hemianopia: a key role for parietal-frontal disconnection? Neuroreport 14:2239–2243

Doricchi F, Thiebaut de Schotten M, Tomaiuolo F, Bartolomeo P (2008) White matter (dis)connections and gray matter (dys)functions in visual neglect: gaining insights into the brain networks of spatial awareness. Cortex 44:983–995

Duffau H (2009) Does post-lesional subcortical plasticity exist in the human brain? Neurosci Res 65:131–135

Duffau H, Capelle L, Sichez J, Faillot T, Abdennour L, Law Koune JD, Dadoun S, Bitar A, Arthuis F, Van Effenterre R, Fohanno D (1999) Intra-operative direct electrical stimulations of the central nervous system: the Salpêtrière experience with 60 patients. Acta Neurochir 141:1157–1167

Friston KJ, Büchel C (2000) Attentional modulation of effective connectivity from V2 to V5/MT in humans. Proc Natl Acad Sci USA 97:7591–7596

Gaffan D, Hornak J (1997) Visual neglect in the monkey. Representation and disconnection. Brain 120:1647–1657

Gainotti G, D'Erme P, Bartolomeo P (1991) Early orientation of attention toward the half space ipsilateral to the lesion in patients with unilateral brain damage. J Neurol Neurosurg Psychiatr 54:1082–1089

Gauthier L, Dehaut F, Joanette Y (1989) The bells test: a quantitative and qualitative test for visual neglect. Int J Clin Neuropsychol 11:49–53

Golay L, Schnider A, Ptak R (2008) Cortical and subcortical anatomy of chronic spatial neglect following vascular damage. Behav Brain Funct 4:43

Good CD (2001) Cerebral asymmetry and the effects of sex and handedness on brain structure: a voxel-based morphometric analysis of 465 normal adult human brains. NeuroImage 14:685–700

Goodlett CB, Fletcher P, Gilmore JH, Gerig G (2009) Group analysis of DTI fiber tract statistics with application to neurodevelopment. NeuroImage 45:S133–S142

Gosh S, Rao PS, De G, Majumder PP (2007) A nonparametric regression-based linkage scan of rheumatoid factor-IgM using sib-pair squared sums and differences. BMC Proc 1:S99

Hayasaka S, Nichols T (2003) Validating cluster size inference: random field and permutation methods. NeuroImage 20:2343–2356

Heilman KM, Watson RT, Bower D, Valenstein E (1983) Right hemisphere dominance for attention. Rev Neurol (Paris) 139:15–17

Holmes AP, Blair RC, Watson JD, Ford I (1996) Nonparametric analysis of statistic images from functional mapping experiments. J Cereb Blood Flow Metab 16:7–22

Holmes CJ, Hoge R, Collins L, Woods R, Toga AW, Evans AC (1998) Enhancement of MR images using registration for signal averaging. J Comput Assist Tomogr 22:324–333

Husain M, Kennard C (1996) Visual neglect associated with frontal lobe infarction. J Neurol 243:652–657

Husain M, Nachev P (2007) Space and the parietal cortex. Trends Cogn Sci 11:30–36

Husain M, Rorden C (2003) Non-spatially lateralized mechanisms in hemispatial neglect. Nat Rev Neurosci 4:26–36

Jones DK, Symms MR, Cercignani M, Howard RJ (2005) The effect of filter size on VBM analyses of DT-MRI data. NeuroImage 26:546–554

Karnath HO, Fruhmann Berger M, Küker W, Rorden C (2004) The anatomy of spatial neglect based on voxelwise statistical analysis: a study of 140 patients. Cereb Cortex 14:1164–1172

Karnath HO, Rorden C, Ticini LF (2009) Damage to white matter fiber tracts in acute spatial neglect. Cereb Cortex 19:2331–2337

Kinsbourne M (1993) Orientational bias model of unilateral neglect: evidence from attentional gradients within hemispace. In: Robertson IH, Marshall JC (eds) Unilateral neglect: clinical and experimental studies. Lawrence Erlbaum Associates, Hove, pp 63–86

Koch G, Oliveri M, Cheeran B, Ruge D, Lo Gerfo E, Salerno S, Torriero S, Marconi B, Mori F, Driver J, Rothwell JC, Caltagirone C (2008) Hyperexcitability of parietal-motor functional connections in the intact left-hemisphere of patients with neglect. Brain 131:3147–3155

Kunimatsu A, Aoki S, Masutani Y, Abe O, Hayashi N, Mori H, Masumoto T, Ohtomo K (2004) The optimal trackability threshold of fractional anisotropy for diffusion tensor tractography of the corticospinal tract. Magn Reson Med Sci 3:11–17

Leibovitch FS, Black SE, Caldwell CB, Ebert PL, Ehrlich LE, Szalai JP (1998) Brain-behavior correlations in hemispatial neglect using CT and SPECT: the Sunnybrook stroke study. Neurology 50:901–908

Losier BJ, Klein RM (2001) A review of the evidence for a disengage deficit following parietal lobe damage. Neurosci Biobehav Rev 25:1–13

Malhotra P, Parton AD, Greenwood R, Husain M (2006) Noradrenergic modulation of space exploration in visual neglect. Ann Neurol 59:186–190

McIntosh AR, Grady CL, Ungerleider LG, Haxby JV, Rapoport SI, Horwitz B (1994) Network analysis of cortical visual pathways mapped with PET. J Neurosci 14:655–666

Mesulam M (1981) A cortical network for directed attention and unilateral neglect. Ann Neurol 10:309–325

Mesulam M (1985) Principles of behavioral neurology. F.A. Davis, Philadelphia

Mort DJ, Malhotra P, Mannan SK, Rorden C, Pambakian A, Kennard C, Husain M (2003) The anatomy of visual neglect. Brain 126:1986–1997

Nichols TE, Holmes AP (2002) Nonparametric permutation tests for functional neuroimaging: a primer with examples. Hum Brain Mapp 15:1–25

Nobre AC (2001) The attentive homunculus: now you see it, now you don't. Neurosci Biobehav Rev 25:477–496

Park KC, Lee BH, Kim EJ, Shin MH, Choi KM, Yoon SS, Kwon SU, Chung CS, Lee KH, Heilman KM, Na DL (2006) Deafferentation-disconnection neglect induced by posterior cerebral artery infarction. Neurology 66:56–61

Pisella L, Rode G, Farnè A, Tilikete C, Rossetti Y (2006) Prism adaptation in the rehabilitation of patients with visuo-spatial cognitive disorders. Curr Opin Neurol 19:534–542

Posner MI, Walker JA, Friedrich FJ, Rafal RD (1984) Effects of parietal injury on covert orienting of attention. J Neurosci 4:1863–1874

Reep RL, Corwin JV, Cheatwood JL, Van Vleet TM, Heilman KM, Watson RT (2004) A rodent model for investigating the neurobiology of controlateral neglect. Cogn Behav Neurol 17:191–194

Robertson LC (2003) Binding, spatial attention and perceptual awareness. Nat Rev Neurosci 4:93–102

Robertson IH, Halligan PW, Bergego C, Homberg V, Pizzamiglio L, Weber E, Wilson BA (1994) Right neglect following right hemisphere damage? Cortex 30:199–213

Rodrigo S, Naggara O, Oppenheim C, Golestani N, Poupon C, Cointepas Y, Mangin JF, Le Bihan D, Meder JF (2007) Human subinsular asymmetry studied by diffusion tensor imaging and fiber tracking. AJNR Am J Neuroradiol 28:1526–1531

Rousseaux M, Beis JM, Pradat-Diehl P, Martin Y, Bartolomeo P, Bernati T, Chokron S, Leclercq M, Louis-Dreyfus A, Marchal F, Perennou D, Prairial C, Rode G, Samuel C, Sieroff E, Wiart L, Azouvi P (2001) Presenting a battery for assessing spatial neglect. Norms and effects of age, educational level, sex, hand and laterality. Rev Neurol (Paris) 157:1385–1400

Salmond CH, Ashburner J, Vargha-Khadem F, Connelly A, Gadian DG, Friston K (2002) Distributional assumptions in voxel-based morphometry. NeuroImage 17:1027–1030

Schmahmann JD, Pandya D (2006) Fiber pathways of the brain. Oxford University Press, New York

Shinoura N, Suzuki Y, Yamada R, Tabei Y, Saito K, Yagi K (2009) Damage to the right superior longitudinal fasciculus in the inferior parietal lobe plays a role in spatial neglect. Neuropsychologia 47:2600–2603

Singh-Curry V, Husain M (2009) The functional role of the inferior parietal lobe in the dorsal and ventral stream dichotomy. Neuropsychologia 47:1434–1448

Smith SM, Johansen-Berg H, Jenkinson M, Rueckert D, Nichols T, Miller KL, Robson MD, Jones DK, Klein JC, Bartsch AJ, Behrens TE (2007) Acquisition and voxelwise analysis of multisubject diffusion data with Tract-Based Spatial Statistics. Nat Protoc 2:499–504

Sotak CH (2002) The role of diffusion tensor imaging in the evaluation of ischemic brain injury—a review. NMR Biomed 15:561–569

Taoka T, Morikawa M, Akashi T, Miyasaka T, Nakagawa H, Kiuchi K, Kishimoto T, Kichikawa K (2009) Fractional anisotropy—threshold dependence in tract-based diffusion tensor analysis: evaluation of the uncinate fasciculus in Alzheimer disease. AJNR Am J Neuroradiol 30:1700–1703

Thiebaut de Schotten M, Urbanski M, Duffau H, Volle E, Levy R, Dubois B, Bartolomeo P (2005) Direct evidence for a parietal-frontal pathway subserving spatial awareness in humans. Science 309:2226–2228

Thiebaut de Schotten M, Kinkingnéhun S, Delmaire C, Lehéricy S, Duffau H, Thivard L, Volle E, Levy R, Dubois B, Bartolomeo P (2008) Visualization of disconnection syndromes in humans. Cortex 44:1097–1103

Thiebaut de Schotten M, Ffytche D, Bizzi A, Dell'Acqua F, Allin M, Walshe M, Murray R, Williams SC, Murphy DGM, Catani M (2010) Atlasing location, asymmetry and inter-subject variability of white matter tracts in the human brain with MR diffusion tractography, NeuroImage. doi:10.1016/j.neuroimage.2010.07.055

Thomalla G, Glauche V, Weiller C, Rother J (2005) Time course of wallerian degeneration after ischaemic stroke revealed by diffusion tensor imaging. J Neurol Neurosurg Psychiatry 76:266–268

Tryon WW (2001) Evaluating statistical difference, equivalence, and indeterminacy using inferential confidence intervals: an integrated alternative method of conducting null hypothesis statistical tests. Psychol Methods 6:371–386

Tryon WW, Lewis C (2008) An inferential confidence interval method of establishing statistical equivalence that corrects Tryon's (2001) reduction factor. Psychol Methods 13:272–277

Urbanski M, Thiebaut de Schotten M, Rodrigo S, Catani M, Oppenheim C, Touze E, Chokron S, Meder JF, Levy R, Dubois B, Bartolomeo P (2008) Brain networks of spatial awareness: evidence from diffusion tensor imaging tractography. J Neurol Neurosurg Psychiatry 79:598–601

Vallar G (2001) Extrapersonal visual unilateral spatial neglect and its neuroanatomy. NeuroImage 14:S52–S58

Verdon V, Schwartz S, Lovblad KO, Hauert CA, Vuilleumier P (2010) Neuroanatomy of hemispatial neglect and its functional components: a study using voxel-based lesion-symptom mapping. Brain 133:880–894

Winkler AM, Nichols T, Glahn DC (2008) On non-normality, non-parametric tests and pooling permutations over space for voxel-based morphometry. Poster presented at the congress human brain mapping, Melbourne, Australia